Proceedings of the 2006 IEEE International Conference on Robotics and Automation
Orlando, Florida - May 2006

The Control of Kinematically Constrained Shoulder Complexes: Physiological and Humanoid Examples

Vincent De Sapio[†‡], Katherine Holzbaur[‡], and Oussama Khatib[†]
[†]*Artificial Intelligence Laboratory, Stanford University, Stanford, CA 94305, USA*
[‡]*Neuromuscular Biomechanics Laboratory, Stanford University, Stanford, CA 94305, USA*

***Abstract*— This paper applies a task-level approach to the control of holonomically constrained shoulder models. These models include a biomechanical representation based on human physiology and a robotic design based on a parallel-serial structure. Both models involve complex kinematically coupled motion between the shoulder girdle and the humerus. This coupled motion has a significant impact on the resulting humeral pointing dynamics associated with arm movement. The constrained task-level control approach implemented here characterizes and exploits the kinematically coupled nature of these systems by casting the constrained dynamics into a task-level control framework. Examples are presented which illustrate the effectiveness of this approach.**

***Index Terms*— task-level control, constraints, parallel-serial, biomechanics, shoulder kinematics**

I. Introduction

The biomechanical study of human motion, as well the design of anthropomorphic robotic mechanisms, require faithful representations of human skeletal kinematics. Over the past decade there has been a proliferation of humanoid robotic systems. Human skeletal kinematics has been modeled in these systems at a basic level but some important aspects have been over-simplified or overlooked. While the representation of any skeletal joint as an ideal revolute or spherical joint is only an approximation, it is typically an acceptable one. Exceptions to this include the knee joint which does not rotate about an absolute center, but translates as well, during knee extension [6]. This added complexity, along with the presence of the patella (knee cap), has a significant influence on the generation of muscle moments about the knee. This is an important consideration if one wishes to simulate the human knee or emulate it in a humanoid robot that is to be driven by artificial muscles or cables. Thus, properly addressing the complexity of skeletal kinematics is important for both biomechanical simulations as well as anthropomorphic robot design.

Perhaps the most kinematically complicated subsystem in the human skeletal system is the shoulder complex. While the purpose of the shoulder complex is to produce spherical articulation of the humerus, the resultant motion does not exclusively involve motion of the glenohumeral joint (see *Figure 1*). The shoulder girdle, which is comprised of the clavicle and scapula, connects the glenohumeral joint to the torso and produces some of the motion associated with the overall articulation of the humerus. While this motion is small compared to the glenohumeral motion its impact on overall arm function is significant [12][13]. This impact is not only associated with the influence of the shoulder girdle on the skeletal kinematics of the shoulder complex, but also its influence on the routing and performance of muscles spanning the shoulder. As a consequence, shoulder kinematics is tightly coupled to the behavior of muscles spanning the shoulder. In turn, the action of these muscles (moments induced about the joints) influences the overall musculoskeletal dynamics of the shoulder. This coupling is illustrated in *Figure 2*.

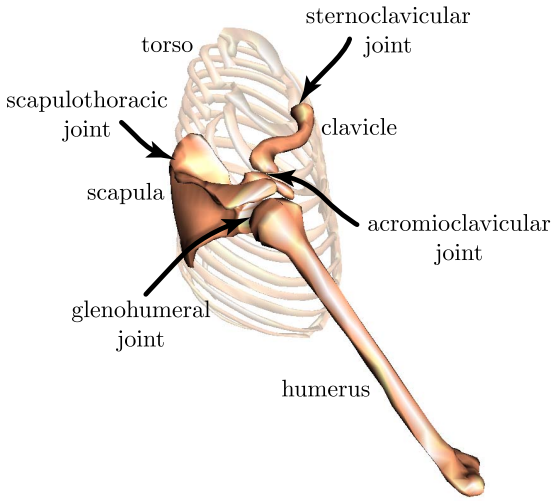

Fig. 1. Various constituents of the shoulder complex including the scapula, clavicle, and humerus. The glenohumeral joint produces spherical motion of the humerus. The shoulder girdle attaches the glenohumeral joint to the torso and influences the resultant motion of the humerus through scapulothoracic, sternoclavicular, and acromioclavicular motion.

For the aforementioned reasons, when modeling the human shoulder it is important to model the kinematically coupled interactions between the shoulder girdle and the glenohumeral joint. This is true for biomechanical simulations as well as for robotic analogs of the human shoulder. To this end, this paper applies a task-level approach to the control of holonomically constrained shoulder models; both human and humanoid. Through this application the novelty and efficacy of the constrained task-level approach is demonstrated with regard to analysis and control of constrained physiological and robotic shoulder complexes.

As a point of departure, a formulation for constrained task-level control is reviewed. Subsequently, this control approach is applied to a physiological model of the human shoulder. In this case, emphasis is placed on exploiting the benefits of constrained task-level control for biome-

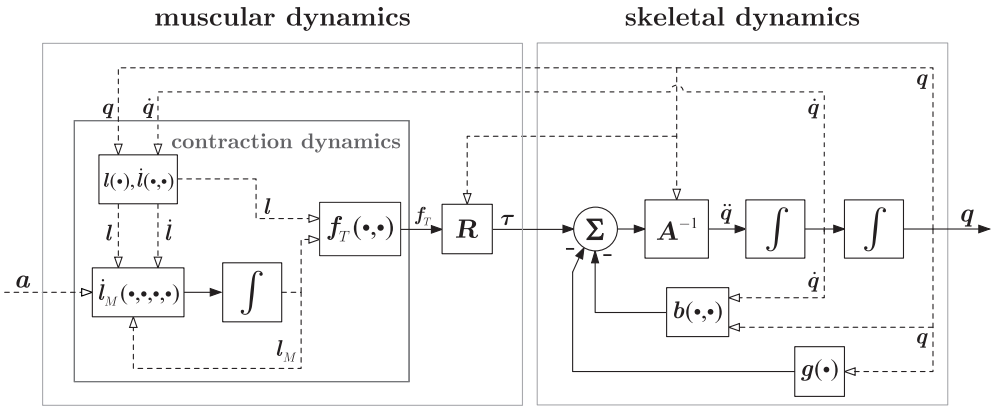

Fig. 2. The dependency of musculoskeletal dynamics on muscle routing and skeletal kinematics. Muscle activation inputs, $\boldsymbol{a}$, cause force generation in the muscles. Force generation, $\boldsymbol{f}_T$, is dependant on muscle length, contraction velocity, and musculotendon length ($\boldsymbol{l}_M$, $\dot{\boldsymbol{l}}_M$, and $\boldsymbol{l}$), which in turn are dependant on skeletal configuration ($\boldsymbol{q}$ and $\dot{\boldsymbol{q}}$). The muscle induced joint moments, $\boldsymbol{\tau}$, are dependent on these muscle forces as well as muscle moment arms, $\boldsymbol{R}$, (which again are dependent on skeletal kinematics). Finally, these joint moments influence the multibody dynamics of the skeletal system.

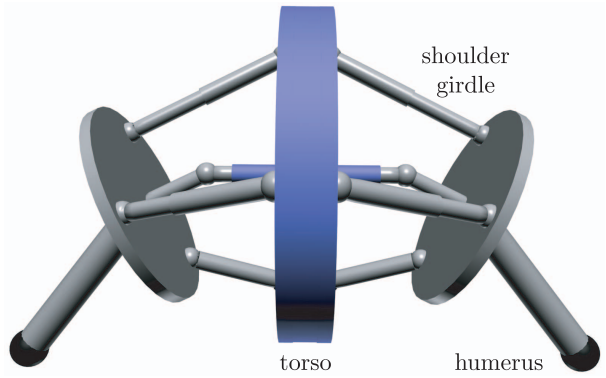

Fig. 3. Bilateral representation of the shoulder complex proposed by Lenarčič et al. [13]. The parallel mechanism shoulder girdle is attached to a fixed torso. The humerus link is attached to the shoulder girdle via a spherical glenohumeral joint.

chanical simulation. A comparison is made between the constrained shoulder model and a simple variant with only glenohumeral articulation. This comparison addresses the control torques required to achieve a desired motion control objective as well as the moment generating capacities of the muscles in both the constrained and simple variants.

Lastly, the constrained task-level control approach is applied to a model of a humanoid shoulder complex. In this case emphasis is placed on exploiting the benefits of constrained task-level control for the control of a redundant parallel-serial shoulder design (see *Figure 3*). Constrained task-level control is particularly well suited not only to simulating such a system but also for implementation in hardware.

II. Constrained Dynamics and Control

Given a set of m_C holonomic constraint equations, $\boldsymbol{\phi} = \boldsymbol{0}$, the constrained equations of motion are given by,

$$\boldsymbol{\tau} = \boldsymbol{A}\ddot{\boldsymbol{q}} + \boldsymbol{b} + \boldsymbol{g} - \boldsymbol{\Phi}^T\boldsymbol{\lambda} \tag{1}$$

subject to the constraint equations. The term $\boldsymbol{\tau}$ is the $n \times 1$ vector of externally applied generalized forces (torques), $\boldsymbol{A}(\boldsymbol{q})$ is the $n \times n$ mass matrix, $\boldsymbol{b}(\boldsymbol{q}, \dot{\boldsymbol{q}})$ is the $n \times 1$ vector of centrifugal-Coriolis terms, and $\boldsymbol{g}(\boldsymbol{q})$ is the $n \times 1$ vector of gravity terms. The constraints are enforced through the Lagrange multipliers, $\boldsymbol{\lambda}$. The $m_C \times n$ constraint matrix, $\boldsymbol{\Phi}$, is given by,

$$\boldsymbol{\Phi}(\boldsymbol{q}) \triangleq \frac{\partial \boldsymbol{\phi}}{\partial \boldsymbol{q}} \tag{2}$$

For conciseness we will often refrain from explicitly denoting the functional dependence of these quantities on $\boldsymbol{q}$ and $\dot{\boldsymbol{q}}$. This practice will also be employed with other quantities throughout the paper.

Given an $m_T \times 1$ task vector, $\boldsymbol{x}_T$, and corresponding $m_T \times n$ task Jacobian, $\boldsymbol{J}_T$, we can map (1) into operational space [9] [10]. This procedure is presented in [4] and the results will be briefly summarized here. The constrained operational space equations of motion resulting from the operational space mapping are,

$$\begin{pmatrix} \boldsymbol{f}_T \\ \boldsymbol{f}_C \end{pmatrix} + \begin{pmatrix} \boldsymbol{0} \\ \boldsymbol{\lambda} \end{pmatrix} = \boldsymbol{\Lambda}(\boldsymbol{q}) \begin{pmatrix} \ddot{\boldsymbol{x}}_T \\ \boldsymbol{0} \end{pmatrix} + \boldsymbol{\mu}(\boldsymbol{q}, \dot{\boldsymbol{q}}) + \boldsymbol{p}(\boldsymbol{q}) \tag{3}$$

where $\boldsymbol{f}_T$ is the $m_T \times 1$ task component and $\boldsymbol{f}_C$ is the $m_C \times 1$ constraint component of the applied operational space force vector. The term $\boldsymbol{\Lambda}(\boldsymbol{q})$ is the $(m_T + m_C) \times (m_T + m_C)$ operational space mass matrix, $\boldsymbol{\mu}(\boldsymbol{q}, \dot{\boldsymbol{q}})$ is the $(m_T + m_C) \times 1$ operational space centrifugal-Coriolis force vector, and $\boldsymbol{p}(\boldsymbol{q})$ is the $(m_T + m_C) \times 1$ operational space gravity vector. These terms are computed from $\boldsymbol{J}_T$ and $\boldsymbol{\Phi}$, and are detailed in [4].

To account for certain joints being unactuated we impose the following condition,

$$\tilde{\boldsymbol{S}}(\boldsymbol{J}_T^T\boldsymbol{f}_T + \boldsymbol{\Phi}^T\boldsymbol{f}_C) = \boldsymbol{0} \tag{4}$$

where $\tilde{\boldsymbol{S}}$ is a selection matrix for the unactuated joints. That is, $\tilde{\boldsymbol{S}}$ selects the unactuated joints from the overall generalized force vector.

By partitioning (3) and using estimates of the operational space dynamic properties we have the following dynamic

compensation equation,

$$\boldsymbol{f}_T = \widehat{\boldsymbol{\Lambda}}_{11}\boldsymbol{f}_T^{\star} + \widehat{\boldsymbol{\mu}}_1 + \widehat{\boldsymbol{p}}_1 \tag{5}$$

where $\boldsymbol{f}_T^{\star}$ is the input of the decoupled system and can be chosen as,

$$\boldsymbol{f}_T^{\star} = \boldsymbol{K}_p(\boldsymbol{x}_{T_d} - \boldsymbol{x}_T) + \boldsymbol{K}_v(\dot{\boldsymbol{x}}_{T_d} - \dot{\boldsymbol{x}}_T) + \ddot{\boldsymbol{x}}_{T_d} \tag{6}$$

The constraint force control term, $\boldsymbol{f}_C$, can be resolved by using,

$$\boldsymbol{f}_C + \boldsymbol{\lambda} = \widehat{\boldsymbol{\Lambda}}_{21}\boldsymbol{f}_T^{\star} + \widehat{\boldsymbol{\mu}}_2 + \widehat{\boldsymbol{p}}_2 \tag{7}$$

in the case that the control is chosen with regard to optimizing the resulting constraint forces, or, by using (4) in order to account for certain joints being unactuated. The overall control torque is given by,

$$\boldsymbol{\tau} = \boldsymbol{J}_T^T\boldsymbol{f}_T + \boldsymbol{\Phi}^T\boldsymbol{f}_C \tag{8}$$

III. Human Shoulder Model

A. Model and Control Implementation

The upper extremity model of Holzbaur et al. [8] has been employed in this work. The model consists of a shoulder complex as well as a lower arm model. Holzbaur et al. implemented their model in the SIMM (**S**oftware for **I**ntegrated **M**usculoskeletal **M**odeling) environment [7] where a minimal set of 7 generalized coordinates were chosen to describe the configuration of the shoulder complex, elbow, and wrist (3 for the shoulder complex, 2 for elbow flexion and pronation, and 2 for wrist flexion and deviation). Since a minimal set of coordinates were employed in [8] the constraints that model the shoulder girdle are implicitly handled. Thus, all motions of the shoulder girdle are dependent on the three glenohumeral rotation coordinates. These are elevation plane, h_1, elevation angle, h_2, and shoulder rotation, h_3.

The constrained movement of the shoulder girdle was determined from the shoulder rhythm regression analysis of de Groot and Brand [3]. The model obtained from this regression analysis was shown to fit well for an independent set of shoulder motions and on a different set of subjects than was used for the regression analysis [3]. For these reasons the model of de Groot and Brand is considered to be superior in predicting shoulder motion than a simple unconstrained model which only reflects glenohumeral rotation.

Due that fact that SIMM restricts any joint motion to a function of a single independent generalized coordinate, the regression equations were simplified by Holzbaur et al. to be a function of only thoracohumeral (humerus elevation) angle, h_2, [8]. The shoulder kinematics for this parameterization are shown in *Table I*.

The terms $\boldsymbol{d}_1$, $\boldsymbol{d}_2$, and $\boldsymbol{d}_3$ are fixed translation vectors and $\boldsymbol{Q}_1, \cdots, \boldsymbol{Q}_7$ are rotation matrices associated with spins about successive local coordinate axes, where the arguments identify the spin angles. The superscript t refers to the torso as the frame of reference. The constraint constants, $\boldsymbol{c}$, associated with the dependency on humerus elevation angle, h_2, were obtained from the regression analysis of de Groot and Brand [3]. They are,

Translation	Rotation
clavicle	
${}^t\boldsymbol{d}_c = \boldsymbol{d}_1$	${}^t_c\boldsymbol{Q} = \boldsymbol{Q}_1(c_1h_2)\boldsymbol{Q}_2(c_2h_2)$
scapula	
${}^t\boldsymbol{d}_s = {}^t\boldsymbol{d}_c + {}^t_c\boldsymbol{Q}\boldsymbol{d}_2$	${}^t_s\boldsymbol{Q} = \boldsymbol{Q}_3(c_3h_2)\boldsymbol{Q}_4(c_4h_2)\boldsymbol{Q}_5(c_5h_2)$
humerus	
${}^t\boldsymbol{d}_h = {}^t\boldsymbol{d}_s + {}^t_s\boldsymbol{Q}\boldsymbol{d}_3$	${}^t_h\boldsymbol{Q} = \boldsymbol{Q}_6(h_1)\boldsymbol{Q}_7(h_2)\boldsymbol{Q}_6(-h_1)\boldsymbol{Q}_6(h_3)$

TABLE I
SHOULDER KINEMATICS USING A MINIMAL SET OF COORDINATES.

$$\boldsymbol{c} = \begin{pmatrix} -0.242 & 0.123 & -0.049 & 0.396 & 0.184 \end{pmatrix}$$

For the purposes of formulating the dynamics and control it is often preferable to use a non-minimal, but standardized, set of generalized coordinates that are amenable to numerical formulation. Additionally, it is preferable to use a parameterization which preserves the physical meaning of the generalized forces as torques about individual joints. Often when using a minimal set of coordinates this is not the case since a single generalized coordinate may influence multiple joint rotations, as in the parameterization of [8].

For these reasons we reparameterized the model of [8] to include a total of $n = 13$ generalized coordinates (9 for the shoulder complex and 4 for the elbow and wrist) to describe the unconstrained configuration of the arm. As shown in *Figure 4*, the coordinates q_6, q_7, and q_9 correspond to the independent coordinates for the shoulder complex used in [8]; elevation plane, elevation angle, and shoulder rotation, respectively.

Five holonomic constraints need to be imposed to properly constrain the motion of the shoulder girdle. With an additional constraint at the glenohumeral joint we have a total of $m_C = 6$ constraints. This yields $p = n - m_C = 7$ degrees of kinematic freedom (3 for the shoulder complex and 4 for the elbow and wrist). Since this framework does not limit the dependent coordinates to functions of only a single independent coordinate, as in the case of the SIMM model [8], we can implement the complete set of shoulder rhythm constraints [3] for our analysis. These constraint equations, $\boldsymbol{\phi}(\boldsymbol{q}) = \boldsymbol{0}$, are given by.

$$\boldsymbol{\phi}(\boldsymbol{q}) = \begin{pmatrix} q_1 - b_1q_6 - c_1q_7 \\ q_2 - b_2q_6 - c_2q_7 \\ q_3 - b_3q_6 - c_3q_7 \\ q_4 - b_4q_6 - c_4q_7 \\ q_5 - b_5q_6 - c_5q_7 \\ q_8 + q_6 \end{pmatrix} = \boldsymbol{0} \tag{9}$$

where the constraint constants, $\boldsymbol{b}$, associated with the dependency on elevation plane, q_{11}, were obtained from the regression analysis [3]. They are,

$$\boldsymbol{b} = \begin{pmatrix} 0.120 & -0.046 & 0.140 & -0.079 & -0.028 \end{pmatrix}$$

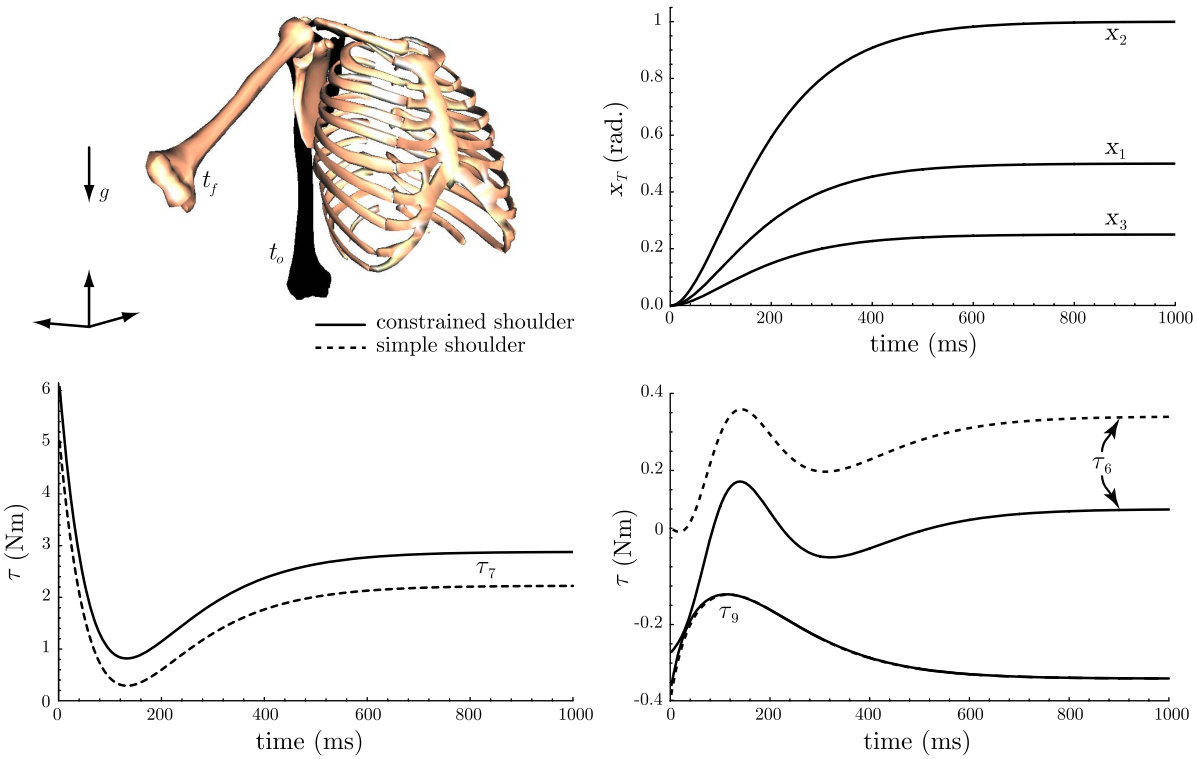

Fig. 5. (Top) Time response of humeral pointing during execution of a goal command for constrained and simple shoulder models. Appropriate dynamic compensation accounts for the control task, $\boldsymbol{x}_T$, and the shoulder girdle constraints, $\boldsymbol{\phi}$. The control gains are $K_p = 100$ and $K_v = 20$. (Bottom) Glenohumeral joint control torques as predicted by the constrained and simple shoulder models. The inclusion of shoulder girdle constraints influences the resulting torques, particularly for shoulder elevation angle and elevation plane.

Defining a humeral orientation, or pointing, task we have,

$$\boldsymbol{x}_T(\boldsymbol{q}) = \begin{pmatrix} q_6 & q_7 & q_9 \end{pmatrix}^T \tag{10}$$

We need to specify a selection matrix, $\tilde{\boldsymbol{S}}$, to account for the unactuated (passive) joints, $q_1, \cdots, q_5$, and q_8. Using the control framework presented in *Section II* we have the control equations,

$$\begin{aligned} \boldsymbol{f}_T &= \boldsymbol{\Lambda}_{11}\ddot{\boldsymbol{x}}_T + \boldsymbol{\mu}_1 + \boldsymbol{p}_1 \\ \tilde{\boldsymbol{S}}(\boldsymbol{J}_T^T\boldsymbol{f}_T + \boldsymbol{\Phi}^T\boldsymbol{f}_C) &= \boldsymbol{0} \\ \boldsymbol{\tau} &= \boldsymbol{J}_T^T\boldsymbol{f}_T + \boldsymbol{\Phi}^T\boldsymbol{f}_C \end{aligned} \tag{11}$$

Figure 5 displays simulation plots for the shoulder complex under a goal position command. A linear (PD) control law is used as the input of the decoupled system. The controller was applied to both the constrained shoulder model and a simple model with only glenohumeral articulation (motion of the scapula and clavicle not coupled to glenohumeral motion). The glenohumeral joint control torques associated with the constrained and simple shoulder models performing identical humeral pointing tasks differ over their respective time histories. This is particularly true for shoulder elevation angle and elevation plane.

B. Muscle-based Actuation

In biomechanical simulations it is desirable to actuate the constrained shoulder complex using a system of musculotendon actuators. Lumped parameter models for muscle-tendon pairs yield equations of state which describe musculotendon behavior [17]. Given a set of r musculotendon actuators we can express the vector of musculotendon forces as $\boldsymbol{f}_T = \boldsymbol{f}_T(\boldsymbol{l}_M, \dot{\boldsymbol{l}}_M, \boldsymbol{a})$, where $\boldsymbol{l}_M$ are the muscle lengths whose behavior is described by a state equation. By using either a stiff tendon model [5] or a steady state evaluation of the musculotendon forces we can express $\boldsymbol{f}_T = \boldsymbol{f}_T(\boldsymbol{q}, \dot{\boldsymbol{q}}, \boldsymbol{a})$. In either case the joint moments induced by these musculotendon forces are,

$$\boldsymbol{\tau} = \boldsymbol{R}(\boldsymbol{q})\boldsymbol{f}_T = -\boldsymbol{L}(\boldsymbol{q})^T\boldsymbol{f}_T \tag{12}$$

where $\boldsymbol{L}(\boldsymbol{q})$ is the $r \times n$ musculotendon path Jacobian and $\boldsymbol{R}(\boldsymbol{q}) = -\boldsymbol{L}^T$ is the $n \times r$ matrix of musculotendon moment arms. Equation (1) can thus be expressed in terms of muscle actuation,

$$\boldsymbol{R}\boldsymbol{f}_T(\boldsymbol{q}, \dot{\boldsymbol{q}}, \boldsymbol{a}) + \boldsymbol{\Phi}^T\boldsymbol{\lambda} = \boldsymbol{A}\ddot{\boldsymbol{q}} + \boldsymbol{b} + \boldsymbol{g} \tag{13}$$

The operational space form is,

$$\boldsymbol{T}(\boldsymbol{q})\boldsymbol{f}_T(\boldsymbol{q}, \dot{\boldsymbol{q}}, \boldsymbol{a}) + \begin{pmatrix} \boldsymbol{0} \\ \boldsymbol{\lambda} \end{pmatrix} = \boldsymbol{\Lambda}\begin{pmatrix} \ddot{\boldsymbol{x}}_T \\ \boldsymbol{0} \end{pmatrix} + \boldsymbol{\mu} + \boldsymbol{p} \tag{14}$$

where $\boldsymbol{T}(\boldsymbol{q}) = \bar{\boldsymbol{J}}^T\boldsymbol{R} \in \mathbb{R}^{(m_T+m_C)\times r}$. Our motion control equation can then be expressed as a variation of (5),

$$\boldsymbol{T}_1\boldsymbol{f}_T(\boldsymbol{q}, \dot{\boldsymbol{q}}, \boldsymbol{a}) = \widehat{\boldsymbol{\Lambda}}_{11}\boldsymbol{f}_T^\star + \widehat{\boldsymbol{\mu}}_1 + \widehat{\boldsymbol{p}}_1 \tag{15}$$

where $\boldsymbol{T}_1$ is the $m_T \times r$ submatrix of $\boldsymbol{T}$. Due to both kinematic redundancy and actuator redundancy there will

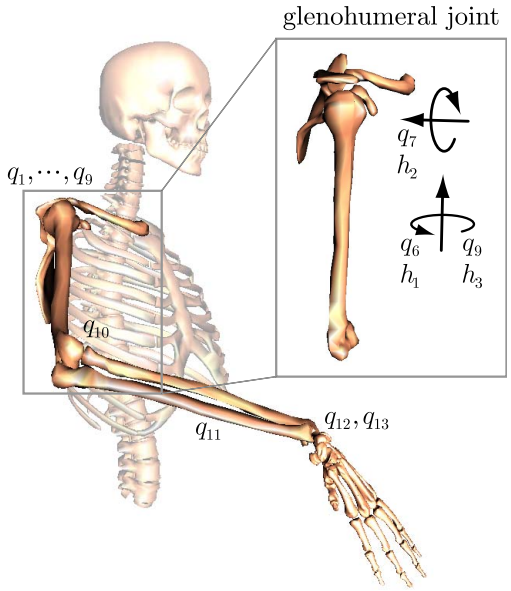

Fig. 4. Reparameterization of the model of Holzbaur et al. Using a non-minimal set coordinates, q_6, q_7, and q_9, correspond to the glenohumeral rotations, h_1, h_2, and h_3. Five holonomic constraints couple the movement of the shoulder girdle with the glenohumeral rotations.

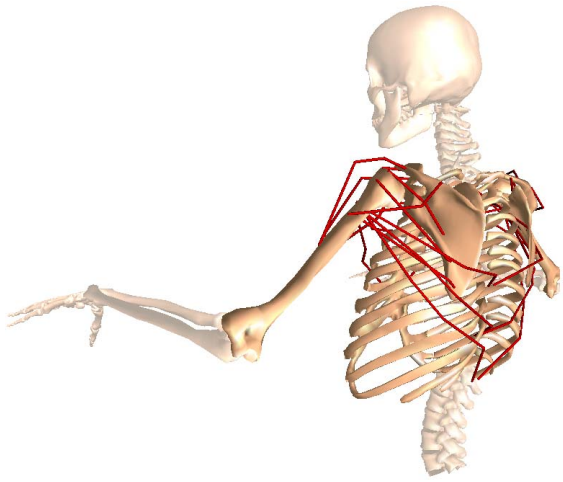

Fig. 6. Muscle paths spanning the shoulder complex. Muscle moment arms are determined from the muscle path data [8]. The motion of the shoulder girdle influences the moment arms about the glenohumeral joint.

typically be many solutions for $\boldsymbol{a}$. Using a static optimization procedure [16] this can be resolved by finding the solution which minimizes $\|\boldsymbol{a}\|^2$ given $\boldsymbol{a} \in [0, 1]$. This corresponds to minimizing the instantaneous muscle effort. The use of $\|\boldsymbol{a}\|^2$ and similar cost measures have been suggested in a number of sources [1][2]. Since muscle activation is a normalized quantity it reflects a natural measure for muscles with different strength capacities.

In *Section III-A* we observed that the constrained shoulder model, which involves kinematic coupling between the humerus, scapula and clavicle, differs from the simple shoulder model with regard to the control torques that are required to achieve a desired motion control task. The constrained model also differs from the simple model in the degree to which the system of muscles are able to generate control forces to achieve a desired motion control task. This is due to the influence of the constrained motion between the humerus, scapula and clavicle on the muscle forces and muscle moment arms about the glenohumeral joint (see *Figure 6*).

An example of this is shown in *Figure 7*. Predicted muscle moment arms, muscle forces, and moment generating capacities for the deltoid muscles are compared for the simple and constrained shoulder models. The muscle path and force-length data were taken from the study of [8]. In the constrained shoulder model the motions of the scapula and clavicle are highly coupled to humerus elevation angle (q_7 coordinate), whereas, in the simple shoulder model the motion of the scapula and clavicle are not coupled to glenohumeral motion. The paths of the deltoid muscles are affected by the constrained motion of the humerus, scapula, and clavicle. This results in significant differences in moment arms predicted by the two models, with the constrained model often generating moment arms of substantially larger magnitude than the simple model.

Additionally the predicted isometric muscle forces (computed at full activation) generated by the two models differ. The resulting moment generating capacities of the constrained model are often substantially larger in magnitude than the simple model. This implies that the simple model, which excludes the constrained shoulder girdle motion, typically underestimates the moment generating capacities of muscles that span the shoulder, since [8] demonstrated correlation between predicted and experimental moment generating capacities for the constrained model. This is critical in various application areas involving the study and synthesis of human movement [11].

IV. Humanoid Robotic Shoulder Complex

The purpose of the biomechanical human shoulder model discussed in the previous section is to simulate physiological shoulder motion and musculotendon routing. As such, it is ultimately intended to be actuated in a physiological manner, that is, by a system of musculotendon actuators that simulate skeletal muscle. For robotic applications, a mechanical analog of the human shoulder may be sought. If this mechanical analog is to be actuated by artificial muscles or cables it is desirable to emulate human shoulder kinematics and muscle routing in order reproduce the human-like action of muscles (moment arms) about the joints.

Standard robotic actuation may be adapted to a humanoid robotic shoulder complex, rather than actuation that attempts to emulate musculoskeletal physiology. This offers the advantages of human shoulder kinematics without requiring complicated actuation. An example of such a system is the shoulder complex proposed by Lenarčič et al. [13] [14]. Their mechanism consists of a parallel-serial

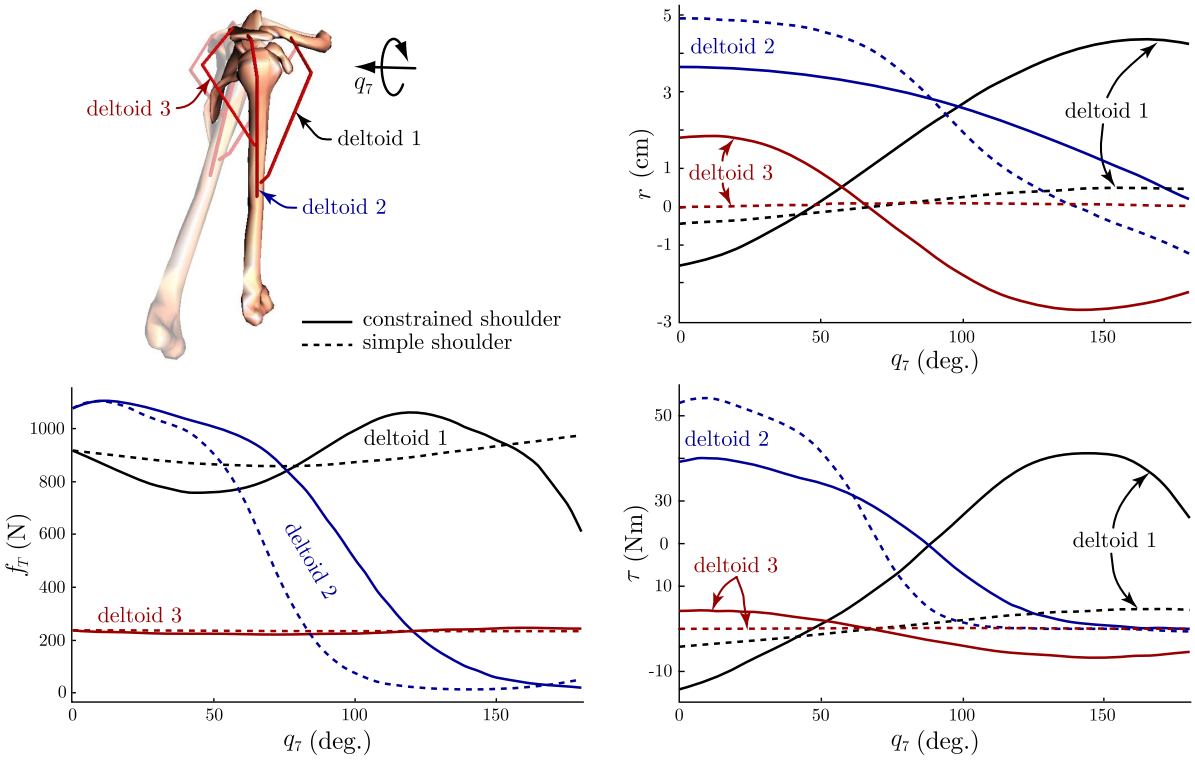

Fig. 7. Muscle moment arms, muscle forces, and moment generating capacities for the deltoid muscles, as predicted by the constrained and simple shoulder models. The constrained model typically generates moment arms of substantially larger magnitude than those of the simple model. The resulting moment generating capacities associated with the constrained model are also typically larger in magnitude than those associated with the simple model.

kinematic structure with four actuated prismatic joints (parallel subsystem) and three actuated revolute joints (serial subsystem).

The parallel subsystem, consisting of four extensible legs attached to a moveable platform, acts as the shoulder girdle which supports the glenohumeral joint. As such, its design is intended to emulate the functionality of the scapula and clavicle attached to a fixed torso and connected by the scapulothoracic, sternoclavicular, and acromioclavicular joints. A parallel kinematic structure was chosen because of the need for high stiffness and precision in orienting the attached glenohumeral joint [13]. The serial subsystem consists of a spherical glenohumeral joint attaching the humerus link to the shoulder girdle.

A. *Model and Control Implementation*

Lenarčič et al. presented detailed kinematic analyses of their shoulder complex design. For our purposes we will present a kinematic parameterization and constraint definition suitable for use in our constraint based control framework. The system is partitioned into four serial chains with a total of 16 generalized coordinates defined as shown in *Figure 8*. Holonomic loop constraints need to be imposed which reflect the connection of the extensible legs to the moveable platform. These constraints are expressed as,

$$\boldsymbol{\phi}(\boldsymbol{q}) = \begin{pmatrix} \boldsymbol{r}_{l_1} - \boldsymbol{r}_{p_1} \\ \boldsymbol{r}_{l_2} - \boldsymbol{r}_{p_2} \\ \boldsymbol{r}_{l_3} - \boldsymbol{r}_{p_3} \end{pmatrix} = \boldsymbol{0} \qquad (16)$$

With these constraints the system possesses $p = n - m_C = 16 - 9 = 7$ degrees of freedom (4 for the parallel subsystem and 3 for the serial subsystem).

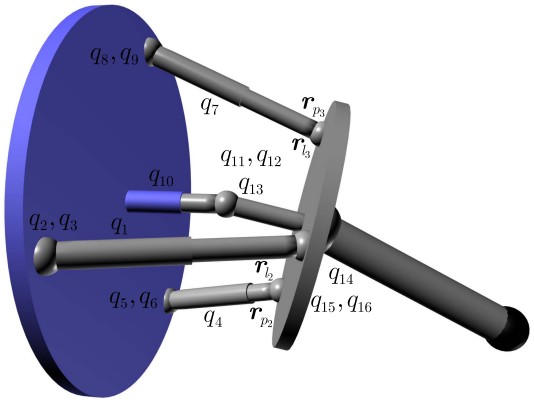

Fig. 8. The parallel and serial subsystems comprising the humanoid shoulder complex proposed by Lenarčič et al. A total of 16 generalized coordinates are employed ($n = 16$). These are constrained by 9 holonomic constraints ($m_T = 9$) yielding 7 degrees of freedom ($p = 7$).

The humanoid shoulder complex is intended to be controlled by $k = 7$ actuators. The actuated joints consist of the four extensible legs and the three glenohumeral rotations. The typical task to be controlled is humeral orientation or pointing, which consists of three task coordinates (for example, Euler angles).

In addition to these control coordinates Lenarčič et al.

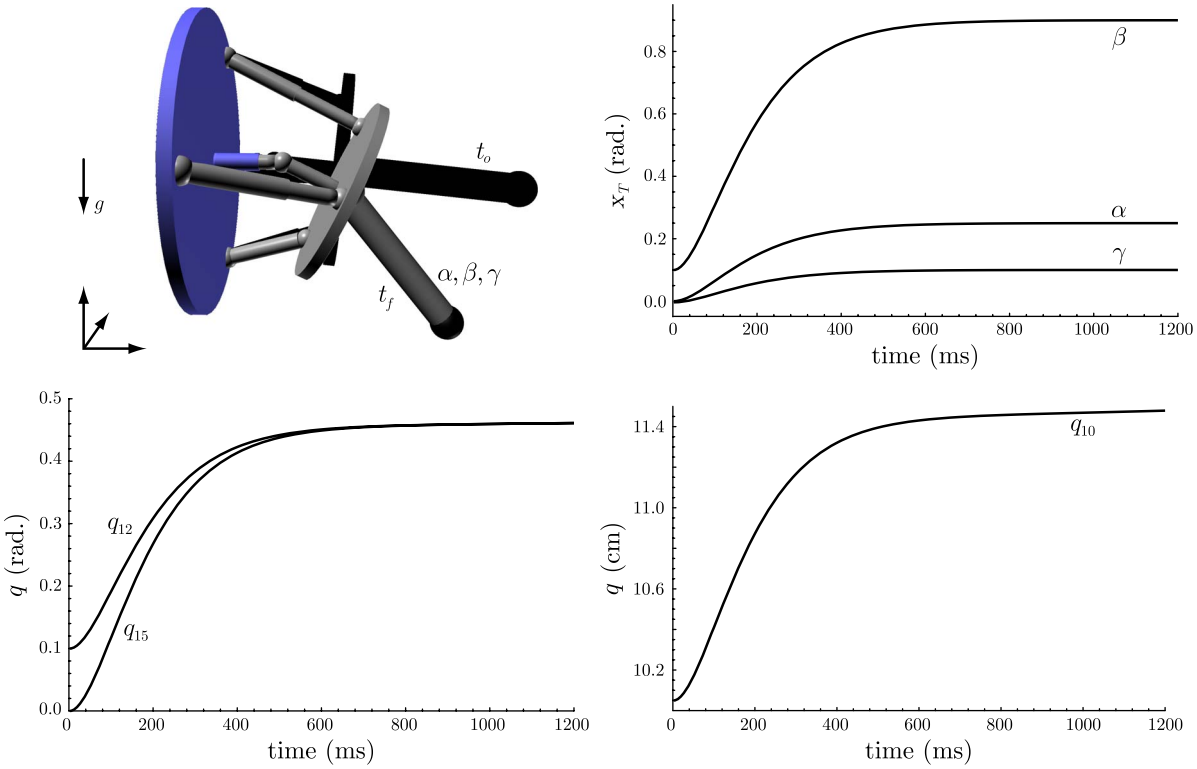

Fig. 9. (Top) Time response of humeral pointing during execution of a goal command. Appropriate dynamic compensation accounts for the control task, $\boldsymbol{x}_T$, and the shoulder girdle loop constraints, $\boldsymbol{\phi}$. The command specifies the desired humeral Euler angles, α, β, and γ using a zyx sequence. (Bottom) Two additional task coordinates are controlled as well. Time response of central leg extension, q_{10}, shoulder girdle pose angle, q_{12}, and glenohumeral rotation angle, q_{15}. These coordinates are coupled through the control task, $\boldsymbol{x}_T$, which causes q_{15} to track q_{12}, and q_{10} to vary as a function of q_{12}. A 2-dimensional null space ($N = 2$) complements the task. The control gains are $K_p = 100$ and $K_v = 20$.

specify physiological coupling between the configuration coordinates. Specifically, the central extensible leg and glenohumeral rotation are intended to vary as a function of the pose of the shoulder girdle. We will specify this coupling in a somewhat arbitrary manner here but the particular nature of this coupling should be derived from measurements of human subjects performing humeral pointing. The overall task vector is of dimension $m_T = 5$ and is specified as,

$$\boldsymbol{x}_T(\boldsymbol{q}) = \begin{pmatrix} \alpha \\ \beta \\ \gamma \\ q_{12} - q_{15} \\ q_{10} - \frac{1}{10}(1 + q_{12}/\pi) \end{pmatrix} = \begin{pmatrix} \alpha_G \\ \beta_G \\ \gamma_G \\ 0 \\ 0 \end{pmatrix} \quad (17)$$

where α, β, and γ are the Euler angles representing humeral orientation using a zyx axis sequence. The subscript G represents the goal values for these quantities. The last two elements in the task vector correspond to the physiological control coupling constraints.

We need to specify a selection matrix, $\tilde{\boldsymbol{S}}$, to account for the unactuated (passive) joints, q_2, q_3, q_5, q_6, q_8, q_9, q_{11}, q_{12}, and q_{13}. Equations (11) can then be implemented as in *Section III-A*.

Figure 9 displays simulation plots for the shoulder complex under a goal position command. A linear (PD) control law is used as the input of the decoupled system. There is an $N = p - m_T = 2$ dimensional null space (self motion manifold) whose control is not specified.

V. Conclusions

In this paper a constrained task-level control approach has been implemented for the simulated control of physiological and robotic shoulder complexes. In the case of the physiological shoulder complex it has been demonstrated that modeling the constrained behavior between the human shoulder girdle and the glenohumeral joint is important in reproducing the appropriate control torques required for achieving a motion control task. It has also been demonstrated that modeling the constrained behavior in the shoulder girdle is important in generating appropriate muscle moment arms, muscle force capacities, and muscle moment capacities about the glenohumeral joint.

For biomechanical simulations this provides a justification for the use of constrained versus simple shoulder models which characterize only glenohumeral rotation. Given this justification, the constrained task-level control approach implemented here is particularly well suited to simulating systems which involve complex kinematically coupled behavior. Such a control implementation is valuable in both evaluating the effect of the kinematic coupling in the shoulder girdle as well as providing a general purpose tool for the biomechanical simulation of these systems.

In the case of the robotic shoulder complex the same basic constrained task-level control framework has been applied to the control of a simulated parallel-serial humanoid shoulder complex. Lenarčič et al., who proposed this basic design made a strong justification for the parallel structure of the shoulder girdle based on the need for high stiffness and precision in orientation. The overall shoulder complex also has the benefit of kinematic redundancy (self motion capability) which allows greater freedom and complexity of achievable motions.

While Lenarčič et al. provided a kinematic analysis of their design no control framework based on the system dynamics was presented. Given the justification for this redundant parallel-serial design, the constrained task-level control approach implemented here has been shown to be very well suited to the control of such a system. This is not only due to its ability to deal with the constraints introduced by the parallel subsystem but also to its ability to easily encode the control in a task-level manner.

ACKNOWLEDGMENT

The authors would like to thank Jaeheung Park, James Warren, Clay Anderson, and Scott Delp for their helpful comments on this work. Vincent De Sapio would also like to thank Sandia National Laboratories for supporting this work.

REFERENCES

[1] F.C. Anderson and M.G. Pandy, "Static and dynamic optimization solutions for gait are practically equivalent," *Journal of Biomechanics*, vol. 34, pp. 153161, 2001.

[2] R.D. Crowninshield and R.A. Brand, "A physiologically based criterion of muscle force prediction in locomotion," *Journal of Biomechanics*, vol. 14, pp. 793801, 1981.

[3] J. H. de Groot and R. Brand, "A three-dimensional regression model of the shoulder rhythm," *Clinical Biomechanics*, vol. 16, pp. 735743, 2001.

[4] V. De Sapio and O. Khatib, "Operational Space Control of Multibody Systems with Explicit Holonomic Constraints," In *Proceedings of the 2005 IEEE International Conference on Robotics and Automation*, vol. 1, pp. 470-475, Barcelona, April 2005.

[5] V. De Sapio, J. Warren, O. Khatib, and S. Delp, "Simulating the Task-level Control of Human Motion: A Methodology and Framework for Implementation," *The Visual Computer*, vol. 21, no. 5, pp. 289302, June 2005.

[6] S. L. Delp, J. P. Loan, M. G. Hoy, F. E. Zajac, E. L. Topp, and J. M. Rosen, "An interactive graphics-based model of the lower extremity to study orthopaedic surgical procedures," *IEEE Transactions on Biomedical Engineering*, vol. 37, pp. 757-767, 1990.

[7] S. L. Delp and J. P. Loan, "A Computational Framework for Simulating and Analyzing Human and Animal Movement," *IEEE Computing in Science and Engineering*, vol. 2, no. 5, pp. 46-55, 2000.

[8] K. R. S. Holzbaur, W. M. Murray, and S. L. Delp, "A Model of the Upper Extremity for Simulating Musculoskeletal Surgery and Analyzing Neuromuscular Control," *Annals of Biomedical Engineering*, vol. 33, no. 6, pp. 829-840, 2005.

[9] O. Khatib, "A Unified Approach to Motion and Force Control of Robot Manipulators: The Operational Space Formulation," *International Journal of Robotics Research*, vol. 3, no. 1, pp. 43-53, 1987.

[10] O. Khatib, "Inertial Properties in Robotic Manipulation: An Object Level Framework," *International Journal of Robotics Research*, vol. 14, no. 1, pp. 19-36, February, 1995.

[11] O. Khatib, J. Warren, V. De Sapio, and L. Sentis, "Human-like motion from physiologically-based potential energies," In Lenarčič J, Galletti C (eds.) *On advances in robot kinematics*, pp. 149–163, Boston: Kluwer, 2004.

[12] N. Klopčar and J. Lenarčič, "Biomechanical Considerations on the Design of a Humanoid Shoulder Girdle," In *Proceedings of the 2001 IEEE/ASME International Conference on Advanced Intelligent Mechatronics*, vol. 1, pp. 255-259, Como, Italy, July 2001.

[13] J. Lenarčič, M. M. Stanišić, and Vincenzo Parenti-Castelli, "Kinematic design of a humanoid robotic shoulder complex," In *Proceedings of the 2000 IEEE International Conference on Robotics and Automation*, vol. 1, pp. 27-32, San Francisco, April 2000.

[14] J. Lenarčič and M. M. Stanišić, "A Humanoid Shoulder Complex and the Humeral Pointing Kinematics," *IEEE Transactions on Robotics and Automation*, vol. 19, no. 3, pp. 499-506, June 2003.

[15] J. Liu, R. E. Hughes, W. P. Smutz, G. Niebur, and K. Nan-An, "Roles of deltoid and rotator cuff muscles in shoulder elevation," *Clinical Biomechanics*, vol. 12, pp. 3238, 1997.

[16] D. G. Thelen, F. C. Anderson, S. L. Delp "Generating dynamic simulations of movement using computed muscle control," *Journal of Biomechanics* vol. 36, pp. 321–328, 2003

[17] F. E. Zajac, "Muscle coordination of movement: a perspective," *Journal of Biomechanics*, vol. 26, pp. 109–124, 1993.